Single-cell transcriptional profiling reveals a novel RAB13^{+} endothelial subpopulation and profibrotic mesenchymal cells in the aged human bone marrow

Itziar Cenzano[1,2,§,*], Miguel Cócera[1,3,4,§], Ana Rosa Lopez-Perez[5], Lorea Campos-Dopazo[1,3], Javier Ruiz[6], Ignacio Sancho[3,6,7], Patxi San Martin-Uriz[1,3], Sarai Sarvide[1], Paula Aguirre-Ruiz[1,3], Amaia Vilas-Zornoza[1], Purificacion Ripalda-Cemborain[1], Diego Alignani[1,4], Aitziber Lopez[1], Marta Miñana Barrios[7], Delia Quilez Agreda[7], Jin Ye[2], Robert Lehmann[2], Laura Sudupe[2], Marta Abengozar-Muela[8], Luis-Esteban Tamariz-Amador[4,9], Emma Muiños-López[1], Borja Saez[1], Jesper Tegner[2,10,11,12], Isabel A. Calvo[1,3,4,*], David Gomez-Cabrero[2,5,*], Felipe Prosper[1,3,4,9,*]

[1]Hematology and Oncology Program, Centre for Applied Medical Research (CIMA), Cancer Center Clinica Universidad de Navarra (CCUN), Pamplona, Navarra, Spain.
[2]Bioscience Program, Biological and Environmental Sciences and Engineering Division (BESE), King Abdullah University of Science and Technology (KAUST), Thuwal, Saudi Arabia.
[3]Instituto de Investigaciones Sanitarias de Navarra (IdiSNA), Spain.
[4]Centro de Investigacion Biomedica en Red de Cancer (CIBERONC). Madrid, Spain.
[5]Translational Bioinformatics Unit, Navarrabiomed, Universidad Pública de Navarra (UPNA).
[6]Hospital Universitario de Navarra, Pamplona, Spain.
[7]Hospital Reina Sofía de Tudela, Navarra, Spain.
[8]Departament of Pathology, Clinica Universidad de Navarra, Pamplona, Spain.
[9]Hematology and Cell Therapy Department. Clínica Universidad de Navarra. Pamplona, Spain.
[10]Computer Science Program, Electrical and Mathematical Sciences and Engineering Division, King Abdullah University of Science and Technology (KAUST), Thuwal, Saudi Arabia.
[11]Unit of Computational Medicine, Department of Medicine, Center for Molecular Medicine, Karolinska Institutet, Karolinska University Hospital, Stockholm, Sweden.
[12]Science for Life Laboratory, Solna, Sweden

[§] These authors contributed equally to this work
* These authors jointly supervised this work

RUNNING TITLE: scRNA-seq transcriptomics of BM microenvironment during aging.

KEYWORDS
Aging, single-cell RNA sequencing, RAB13^{+}, Endothelial cells, Stromal cells, tumor microenvironment, senescence, prothrombotic, profibrotic.

CORRESPONDING AUTHOR
Felipe Prósper (fprosper@unav.es), David Gomez-Cabrero (david.gomezcabrero@kaust.edu.sa), Isabel A. Calvo (icalvoa@unav.es) and Itziar Cenzano (Itziar.cenzano@kaust.edu.sa).

For original data, please contact (Itziar.cenzano@kaust.edu.sa)

ABSTRACT
The bone marrow (BM) microenvironment plays a crucial role in regulating hematopoiesis, yet the molecular and functional changes associated with aging in humans remain poorly understood. Using single-cell RNA sequencing (scRNA-seq), we uncovered transcriptional shifts in BM endothelial cells (EC) and mesenchymal stem cells (MSC) during aging. Our analysis revealed that aged sinusoidal EC adopt a prothrombotic, exhibit mitochondrial dysfunction, and have compromised vascular function. Additionally, we identified a unique arterial EC subset, present only in aged individuals, associated with transcriptional elongation and senescence processes and characterized by *RAB13* expression. MSC from aged subjects displayed an impaired matrix remodeling and epithelial-mesenchymal transition, driven partly by a subpopulation of $THY1^{+}$ profibrotic stromal cells absent in young subjects. Aged MSC were also characterized by an increased ATP-oxidative metabolism and reduced protein folding capacity. Finally, using immunofluorescent imaging and spatial transcriptomics, we confirmed the presence of $RAB13^{+}$ senescent EC in aged samples and revealed significant age-related changes in cell-cell communication within the BM niche. In summary, this work provides a comprehensive view of the molecular diversity, cellular interactions, and spatial organization of aged EC and MSC, offering novel insights and potential targets that could be exploited for preventing aged-associated changes in humans.

INTRODUCTION

Hematopoietic stem cells (HSC) are the fundamental pillar of the hematopoietic system, sustaining blood production for the entire lifespan of an organism[1]. The HSC reside within a specialized bone marrow (BM) microenvironment called niche[2]. The HSC niche consists of a complex and dynamic molecular network of interactions among hematopoietic and non-hematopoietic cells, extracellular matrix (ECM) components, and soluble factors, all working together to ensure proper hematopoiesis[3–5].

Aging induces a progressive decline of the anatomical and physiological function of all organ systems[6] and is the major risk factor across different diseases. In the hematopoietic system, aging is characterized by an increased number of HSC accompanied by reduced self-renewal capacity and regenerative potential [7,8]. Over the past decades, several molecular mechanisms that control the HSC aging process have been revealed, yet our understanding remains incomplete[9,10]. What has been established is that the senescent phenotype results from the combination and interplay of the intrinsic aging of the HSC and the detrimental effects of an aged microenvironment[9,11.] The study of the microenvironment has demonstrated that aging causes a reduction in the number of endothelial cells (EC), significant disorganization of vascular structures, decreased angiogenic potential, and increased vascular leakiness and reactive oxygen species (ROS)[12–16]. Additionally, aged mesenchymal stromal cells (MSC) exhibit impaired differentiation into osteoblasts towards adipocytes and secretion of pro-inflammatory cytokines influencing the skewed myeloid differentiation of aged HSC[17,18]. Therefore, to fully comprehend and possibly mitigate the effects of aging in the hematopoietic system, it is necessary to dissect the complex interactions between aged HSC and their aged non-hematopoietic microenvironment.

In that direction, recent studies have shed light on remodeling the non-hematopoietic BM microenvironment in mice during aging[19,20]. However, translating these findings to humans has been challenging, primarily due to difficulties adapting methodologies from mouse models and obtaining high-quality human samples with adequate EC and MSC populations[21–25]. Consequently, these limitations have restricted the scope of single cell analyses in the non-hematopoietic BM compartment. In this article, we profiled EC and MSC at both single-cell and spatial resolution from human BM samples of young and elderly healthy donors undergoing orthopedic surgery.

Our analysis reveals that aged sinusoidal EC display a prothrombotic profile and impaired mitochondrial and vascular functions. We identify an aged arterial-like EC subset marked by RAB13 expression linked to dysregulated transcriptional elongation activity and cellular senescence process. In the stromal compartment, aging drives matrix remodeling mediated partly by $THY1^+$ profibrotic stromal cells, increased oxidative phosphorylation (OXPHOS), and a reduced unfolded protein response. Furthermore, we explore the spatial context of these alterations using immunofluorescent imaging and spatial transcriptomics. These spatial approaches confirm the presence of $RAB13^+$ senescent EC in aged samples and uncover significant age-related disruptions in cell-cell communication within the BM niche. This comprehensive analysis provides new insights into the transcriptomic alterations occurring with aging in the human BM.

METHODS

Human samples

Human BM samples were obtained from healthy young (ranging between 20 and 48 years of age) and elderly (ranging between 58 and 80 years of age) individuals of both sexes undergoing orthopedic surgery (hip or knee replacement). Samples were collected at Hospital Universitario de Navarra and Hospital Reina Sofía de Tudela. Written informed consent was obtained according to the Declaration of Helsinki and the Institutional Review Board of the University of Navarra. The characteristics of all individuals are described in **Supplementary Table 1**. Endothelial and mesenchymal human non-hematopoietic BM cells were isolated by FACS as previously described[26] for subsequent scRNA-seq analysis (**Extended Data Fig. 1**).

Human BM biopsies from young (34-48 years of age) and aged (72-78 years of age) individuals were obtained from Hospital Universitario de Navarra after obtaining written informed consent (**Supplementary Table 2)**. Archived formalin-fixed paraffin-embedded (FFPE) human BM biopsies of four Myelofibrosis (MF) patients (65–73 years of age) were obtained from the Pathology Department of Clínica Universidad de Navarra (CUN) after written informed consent was achieved (**Supplementary Table 2)**. The Research Ethics Committee of the University of Navarra approved the human sample collection and research conducted in this study. Personal data was kept confidential following the Organic Law 3/2018 on personal data protection and Spanish Law 14/2007 on Biomedical research. All collection samples are codified; only authorized personnel can correlate the patient's identity with the codes. Human BM biopsies were processed for Spatial Transcriptomics (Visium, 10X Genomics) or processed and stained for Hematoxylin-Eosin staining (H&E), Masson's Trichrome, or immunofluorescence (IF).

Single-cell RNA sequencing and bioinformatic analysis
The specifics related to the preparation, sequencing, and analysis of the scRNA-seq libraries, together with specific details of the bioinformatic analysis, including quality control steps, differential expression, gene set enrichment analysis (GSEA), cell-cell communication, and gene regulatory network (GRN) analysis, are described in the supplemental Methods. scRNA-seq genomic sequence reads were treated with the CellRanger suite v 6.1.1 against the human GRCh38 reference genome with default parameters. scRNA-seq analysis was performed using R version (v) 4.1.3 and Seurat v 4.3.0[27].

Spatial transcriptomics analysis
Human bone samples were sequenced and analyzed as previously described[28]. The SpaceRanger pipeline v2.01 (10x Genomics) and the GRCh38-2020 reference were used to process FASTQ files. Spots with low UMI and features were removed from the analysis. Deconvolution was done with CARD[29] using a scRNAseq dataset as a reference[25]. Deconvolution and AUC scores were used to label the spots. For Golden MSC and EC spots, deconvolutions and AUC scores were calculated to determine the specific subtypes. All plots were generated in R using Seurat or STutility packages. Further details are provided in the supplemental methods and the GitHub.

Data and code availability
The scRNA-seq data generated in this study and spatial data from the young sample will be publicly available as of the date of peer-reviewed publication and is available under request, contact (itziar.cenzano@kaust.edu.sa). Spatial raw and processed data from the elderly sample has been deposited at GSE269875. scRNA-seq data used for spatial deconvolution was obtained from GSE253355.

All detailed information is provided in the supplemental methods.

RESULTS

Transcriptional profiling of human young and aged BM endothelial and stromal cells
To investigate age-related changes in the human non-hematopoietic BM microenvironment, we performed single-cell transcriptomics on prospectively FACS-isolated EC and MSC from healthy young (<50 years of age; mean 37,8) and aged (>50 years of age; mean 68,5) individuals undergoing orthopedic surgery (**Fig. 1a, Extended Data Fig. 1 and Supplementary Table 1**). After initial quality control and pre-processing, we obtained a total of 35368 cells across all samples (14283 from young and 21085 from aged individuals), which, despite our sorting strategy, included contaminant hematopoietic cells.

Therefore, we first identified and manually annotated the distinct clusters based on the expression of well-known marker genes (**Fig. 1b-c and Extended Data Fig. 2a-b**). EC (cluster 5, n=2159 cells) were identified based on the expression of endothelial canonical markers such as *FABP4*, *CAV1*, and *VWF* and MSC (clusters 2 and 12, n=5317 cells) based on the expression of MSC and

OLN-primed markers including *CXCL12*, *IGFBP5*, and *COL1A2* (**Extended Data Fig. 2c-d**). The remaining clusters were assigned to well-known hematopoietic BM populations, such as monocytes, granulocyte precursors, erythroblasts, neutrophils, plasma cells (PC), platelets/megakaryocytes, CD8-natural killer-like T cells, dendritic cells (DC), and proB cells, based on their respective marker expressions (**Fig. 1c**). Notably, the post-annotation resulting cell-type-specific signatures summarized in **Supplementary Table 3** can serve as a valuable resource for identifying or isolating cell types within BM resident populations, thereby enabling the development of more precise sorting strategies.

To focus on the cells of interest, we separately analyzed EC and MSC from both age groups. Additional filtering and validation were performed, confirming the identity of EC and MSC based on canonical marker expression (**Extended Data Fig. 2e-f**). In total, our dataset comprised 2163 EC (549 young, 1614 aged cells) and 5470 stromal cells (808 young, 4662 aged cells) (**Fig. 1d-e and Extended Data Fig. 2g-h**). Overall, these results demonstrate the feasibility of using BM samples from orthopedic surgeries to successfully isolate and analyze the transcriptional signatures of low-frequency BM EC and MSC in humans.

Aging is associated with a pro-inflammatory program in EC and emergence of RAB13$^+$ senescence cells

To uncover transcriptional differences between EC from young and aged individuals, we first distinguished the major endothelial vascular beds based on the expression of known molecular markers and gene signatures described in previous murine literature[22,30] (**Fig. 2a and Extended Data Fig. 3a**). Arterial cells were characterized by the expression of *GJA4*, *SEMA3G*, *GLUL,* and *FN1*, whereas sinusoids, overexpressed *CLEC4G*, *MS4A6A*, *SEMA3A*, and *STAB2* (**Extended Data Fig. 3b**). Beyond characterizing arteries and sinusoids, we identified previously unreported vascular beds in the human BM, including capillaries and venous vessels (**Supplementary Table 4**). Capillaries were defined by the significant upregulation of known markers, including *TIMP4*, *APOD*, *CA4,* and *TNFRSF4,* as well as vascular differentiation factors resembling the transitional capillary network (**Extended Data Fig. 3b**). Moreover, the recognized venous cluster showed markers of activated post-capillary venules such as *ACKR1*, *CLU*, and *PLAT*, alongside other genes like *VWF* involved in coagulation and hemostasis[31] (**Extended Data Fig. 3b**). Additionally, we discovered a group of EC in a proliferative state (**Extended Data Fig. 3c**), along with an arterial-like EC subset marked by the expression of *RAB13,* which we designated as RAB13$^+$ cells (**Extended Data Fig. 3d**). The functional specialization of each EC cluster was further characterized using *Gene Ontology biological process* (GO) based overrepresentation analysis (ORA)[32,33] (**Extended Data Fig. 3e).**

Given the diversity of vascular beds, we first examined how aging affects the composition of EC subtypes in the human BM. Our analysis revealed significant age-dependent shifts in EC cluster distribution. Specifically, we observed a reduction in sinusoidal EC and an increase in both the venous EC cluster and the RAB13$^+$ EC subset in aged individuals (**Fig. 2b-c and Extended Data Fig. 4a**). Interestingly, the venous cluster was defined by an increased expression of genes related to "antigen processing and presentation" and "leukocyte activation involved in immune response" (*CD74*, *HLA−DRA*, *HLA−DQB1*, *TFF3*), suggesting an imbalanced immune function and elevated pro-inflammatory response during aging (**Fig. 2d and Extended Data Fig. 4b**). Besides being a marker of the venous cluster, *SELE*, one of the major drivers of prothrombotic endothelial activation and leukocyte extravasation during inflammation[34], was highly expressed in aged venous EC and may serve as a potential biomarker for EC aging (**Fig. 2e and Extended Data Fig. 4c**).

Interestingly, our study identified the emergence of a transcriptionally distinct subset of EC in aged individuals defined by a high expression of *RAB13*, a GTPase associated with cellular senescence[35] (**Fig. 2f, Extended Data Fig. 4d**). These RAB13$^+$ EC exhibited transcriptional similarities to arterial cells but could be distinguished by elevated expression of genes associated with mRNA stability and translation, including *HNRNPA1*, *YBX1*, and *NPM1* (**Fig. 2g and**

Supplementary Table 5). Functional enrichment analysis of RAB13$^+$ cells revealed an upregulation of ribosomal biogenesis with an increased expression of ribosomal binding proteins (RBP) and translation-related processes (**Supplementary Table 5** and **Extended Data Fig. 4e-f**). These findings align with recent studies implicating ribosomes in the aging process[36,37]. In addition, we observed gene sets associated with cellular senescence (*RAB13, VIM*, *SPARC*, *CCND1,* and *NME2)* and Myc targets (*NPM1, HNRNPA1, NAP1L1,* and *EEF1B2*) in RAB13$^+$ cells (**Fig. 2h and Extended Data Fig. 4g**).

To better understand the molecular mechanisms underlying this age-related subset, we identified the active regulons in RAB13$^+$ arterial-like EC population using SCENIC[38] and further bioinformatically validating them in SimiC. Interestingly, our analysis identified the ZEB1 regulon as a candidate master regulator of RAB13$^+$ EC subtype (**Fig. 2i and Extended Data Fig. 4h-i**). The ZEB1 transcription factor (TF) is a known inducer of epithelial-mesenchymal transition (EMT) and has been identified as a critical regulator of HSC self-renewal and differentiation[39]. Moreover, recent evidence suggests that upregulation of ZEB1 maintains quiescence in EC progenitors and muscle stem cells, aiding in muscle regeneration post-injury[40,41].

Altogether, our results identified an elevated inflammatory and prothrombotic response and the emergence of an aging-related EC subset associated with ribosomes, dysregulated transcriptional elongation, and senescence, highlighting the significant remodeling of the human BM vasculature during aging.

Aged sinusoids exhibited mitochondrial dysfunction and impaired vascular functions

In addition to examining changes in the composition of EC subtypes with aging, we aimed to investigate the transcriptional alterations in the human BM endothelium associated with aging. Sinusoids showed the most significant number of differentially expressed genes (DEGs), which may be related to the vascular permeability and leakiness observed in the aged BM[42] (**Fig. 3a and Extended Data Fig. 5a**). Differential expression analysis identified 88 upregulated and 55 downregulated genes in aged sinusoids (**Extended Data Fig. 5b and Supplementary Table 6**). EC exhibited age-related changes that mirror alterations observed in other tissues. Notably, several of these changes contributed to a pro-coagulant state, thereby increasing the risk of thrombosis in the aging population[43,44]. The upregulation of genes such as *ANXA2*, *VWF*, and *PLAT,* among others in aged sinusoids, further supported the hypothesis that age-related endothelial dysfunction underlies the heightened incidence of thrombosis (**Fig. 3b and Extended Data Fig. 5c**). In addition to prothrombotic genes, we also observed elevated expression of genes involved in ECM regulation, including *VIM, GSN*, *IGFBP4, ANXA5,* and *RAMP2* (**Fig. 3b and Extended Data Fig. 5c**). These findings in aged EC aligned with previous studies identifying these genes as potential biomarkers of aging across various cell types and tissues[45,46]. Additionally, aged sinusoids showed upregulation of several genes involved in mitochondrial function and cellular detoxification, such as *ATP5MC2*, *ATP5F1E*, *UQCR11*, *COX4I1*, *COX6A1*, *COX7C*, *NDUFB11,* and *NDUFA11*, reflecting enhanced aging-related dysfunction in cellular respiration (**Extended Data Fig. 5d and Supplementary Table 6)**. Pathway enrichment analysis further revealed that many of these upregulated genes were associated with key hallmarks of aging, including oxidative stress, mitochondrial dysfunction, adipogenesis, and coagulation (**Fig. 3c and Extended Data Fig. 5d, e**).

In contrast, genes involved in epithelial cell proliferation and the regulation of endothelial migration were downregulated in aged sinusoids, indicating age-related vascular dysfunction (**Fig. 3c and Extended Data Fig. 5f**). Interestingly, we also observed downregulation of some solute carriers (*SLC2A3*, *SLC25A37*, *SLC8A1*), supporting a decreased response to metal ions (**Fig. 3d**). This decrease also suggested a diminished capacity of EC to process iron and calcium, potentially contributing to the accumulation of non-organic compounds observed during aging, ultimately leading to cellular damage[47].

GRN analysis revealed a global decline in regulon activity along the aging process (**Fig. 3e**). This decline involves TF such as *CEBPB*, *HES1*, *HMBOX1*, *TGIF2,* and *NR5A2*, which are implicated in various biological processes, including cellular proliferation, vascular development, ion regulation, ERK signaling, and differentiation, among others. These results suggested that the impairment of angiogenic vascular functions could be attributed to decreased activity of key TF in aged sinusoids. Collectively, these findings revealed aging-associated molecular features in human BM EC, highlighting thrombosis, mitochondrial dysfunction, compromised vascular functions, and disrupted solute transport as prominent and potential hallmarks in aged sinusoids.

THY1+-Fibro MSC and matrix remodeling are key factors during BM stromal aging

To explore the age-related transcriptional remodeling of the human BM stroma, we first sought to identify well-established MSC populations in our data based on the expression of established stromal markers[22,25,48,49] (**Fig. 4a**). Undifferentiated MSC were defined by their characteristic signature expressing *CXCL12*, *LEPR*, *VCAM1,* and *CP* (**Fig. 4b**). In contrast, MSC committed to the osteolineage (OLN-primed) exhibited the expression of osteogenic makers, including *BGLAP*, *SPP1*, *RUNX2,* and *NCAM1* (**Fig. 4c**). On the other hand, pericytes showed the expression of specific genes such as *RGS5*, *MCAM*, *NES*, and *FABP4* (**Fig. 4d**). Interestingly, we also identified a population of MSC that highly expressed *THY1*, resembling the stromal Fibro and THY1$^+$ MSC subsets recently found in the human BM data from Bandyopadhyay et al.[25] (**Extended Data Fig. 6a, b**). Consequently, we termed this population THY1$^+$Fibro-MSC (**Fig. 4a**).

To assess the impact of aging on the stromal compartment at the cellular level, we investigated potential changes in the abundance of each cell type between young and aged MSC. Our analysis revealed significant variation in cellular composition among individuals (**Fig. 4e**). Particularly, the presence of pericytes and OLN-primed cells was only seen in specific samples, which may not accurately reflect age-related changes in proportions, possibly associated with variances in tissue location and sample dissociation. Nevertheless, we consistently found THY1$^+$Fibro-MSC in all samples from elderly individuals, suggesting that these cells emerge in the aged BM (**Fig. 4e left panel**). The expansion of these THY1$^+$Fibro-MSC during aging aligns with the identification of this mesenchymal subset by Bandyopadhyay et al.[25], whose cohort comprised elderly individuals, thereby representing an "aged" BM microenvironment (**Fig. 4f**).

To delve into the potential role of THY1$^+$Fibro-MSC as regulators of BM decline during the aging process, we analyzed their transcriptome. We observed increased expression of *FN1*, *MIF*, *S100A6,* and *ANXA2,* suggesting the profibrotic nature of aged MSC (**Extended Data Fig. 6c, Supplementary Table 7)**. These findings aligned with previous evidence observed in other tissues of murine models[50–52]. Besides the expression of multiple genes implicated in ECM organization and cell-matrix interactions, such as *ACTG1*, *ACTA2*, *TPM2*, *TPM4*, and *LGALS1* (**Fig. 4g and Supplementary Table 7**), THY1$^+$Fibro-MSC showed elevated expression of *COL1A1*, *COL3A1,* and *COL1A2*, which are involved in the TGF-β signaling pathway (**Extended Data Fig. 6d**). Interestingly, TGF-β signaling plays a pivotal role in myelofibrosis by promoting BM fibrosis and collagen deposition[53,54]. Moreover, these cells exhibited high expression of key genes implicated in myelofibrosis and other fibrotic disorders, such as *IGFB6* and *IGFB7* (**Extended Data Fig. 6e**)[55,56]. In line with these results, pathway analysis identified significant enrichment in cell-substrate assembly, EMT, ECM organization, and aging, suggesting the implication of this profibrotic state in aged MSC (**Fig. 4h, Extended Data Fig. 6f and Supplementary Table 7**). THY1$^+$Fibro-MSC also presented enrichment in homophilic cell adhesion, suggesting an altered interaction with the marrow environment (**Fig. 4h)**.

To further confirm the changes in MSC between young and elderly BM samples, including the identification of THY1$^+$Fibro stromal cells in aged individuals, we performed immunofluorescence (IF) staining of this population in new formalin-fixed paraffin-embedded (FFPE) young and elderly BM biopsies. An increase in THY1$^+$ cells among aged MSC, identified by CD90$^+$ in PRRX1$^+$ cells, was observed (**Fig. 4i-j and Extended Data Fig. 6g**). In brief, these

results suggest a more fibrotic and less functional aged BM microenvironment potentially contributing to the reduced hematopoietic-supportive capacity in aged BM.

Building on these findings, we hypothesize that THY1$^+$ MSC may contribute to the age-dependent development of fibrosis and may have important implications for BM fibrotic diseases such as myelofibrosis (**Extended Data Fig. 6h**). Using IF staining, we observed an increase of THY1$^+$ MSC, marked by an increase in the number of cells co-expressing CD90 and PRRX1 in the BM of myelofibrosis patients, particularly in scar tissue areas (**Extended Data Fig. 6g and i**). Taken together, the elevated presence of these profibrotic cells in myelofibrosis patients indicates their potential involvement in the replacement of hematopoietic cells with fibrotic tissue. Although functional validation of this hypothesis is necessary, our findings imply that these cells could be key drivers of age-related deterioration of the BM microenvironment and hematopoiesis. Targeting these profibrotic cells could pave the way for novel therapeutic strategies aimed at mitigating age-associated BM dysfunction and preserving hematopoietic health.

Impaired oxidative metabolism and protein folding capacity in aged MSC

To further delve into the different molecular processes underlying stromal aging, we investigated the transcriptional changes between young and aged stromal cells. Undifferentiated MSC showed the largest number of DEGs, demonstrating age-related defects in these mesenchymal progenitors (**Fig. 5a and Extended Data Fig. 7a**). Specifically, differential expression analysis detected 367 DEGs, including 203 upregulated genes and 164 downregulated genes in aged MSC (**Fig. 5b and Supplementary Table 8**). Enrichment analysis revealed that many downregulated genes were linked to ossification-related processes. This suggested that age-related bone loss may stem from impairments in the early stages of differentiation rather than changes in the OLN-committed MSC (**Fig. 5c and Supplementary Table 9**). We also found a downregulation of genes that regulate hematopoiesis and cell differentiation, such as *MEIS2*, *GAS6*, *SMAD7,* and *ID2*, as well as heat-shock proteins and other essential genes mediating the response to protein folding and external stimulus (*HSPA1A*, *HSPA1B*, *NEAT1* and *THBS1* among others) (**Extended Data Fig. 7b-c)**. These results showed that aged MSC may face challenges in maintaining proper hematopoietic function and managing misfolded proteins, potentially contributing to age-related hematopoietic dysfunction and disturbances in proteostasis preservation[57]. Moreover, consistent with previous findings in other tissues, the downregulation of angiogenesis-related terms in aged BM MSC suggests a compromised ability of the mesenchymal progenitors to support BM vascular networks[58].

Additionally, aged MSC showed increased expression of genes associated with OXPHOS and ATP metabolism, including *GSTP1*, *ATP5F1E*, *COX7C*, *NUPR1*, *NDUFA4,* and *CHCHD2*, suggesting an abnormal mitochondrial metabolism with higher OXPHOS activity in aged MSC (**Fig. 5d and Extended Data Fig. 7d-e**). This could be attributed to mitochondrial dysfunction and elevated ROS levels, in line with the reported impairment of mitochondrial complexes in aged MSC[59]. The expression of the adipogenic genes *APOE*, *SPARCL1,* and *CAVIN1,* and several genes involved in ECM organization and remodeling, such as *TAGLN, COL3A1, LGALS1*, *MYL9*, *PTX3, and TIMP3*, was increased with age (**Fig. 5e and Extended Data Fig. 7f**). Accordingly, GSEA revealed enrichment in EMT, OXPHOS and adipogenesis (**Fig. 5f and Extended Data Fig. 7f**). Along with the enhanced EMT process during aging, aged MSC showed decreased expression of metalloproteinases *ADAMTS9* and *ADAMTSL3* further implicating the critical role of the ECM remodeling during BM stromal aging (**Extended Data Fig. 7g**). This aligned with the fact that MSC senescence induces changes in ECM, affecting their repair tissue ability[60].

In summary, our results support the contribution of MSC to the age-related alterations in hematopoiesis. The fact that MSC from aged subjects show a heightened oxidative metabolism, EMT, impaired hematopoietic differentiation, and protein folding capacity along with the presence of THY1$^+$Fibro-MSC clearly supports this hypothesis and establishes the BM niche as a target for anti-aging therapies.

Age-related remodeling of EC-MSC communication
After characterizing the aging-associated changes in individual microenvironment cell types, we aimed to dissect how those alterations may affect cell-cell communication mechanisms. To this end, we conducted a single-cell-based ligand-receptor (L-R) analysis using LIANA (**Supplementary Table 10**). Our initial focus was on interactions between EC and MSC and changes induced by aging in their communication. Globally, we observed a slight reduction in outgoing interactions in both EC and MSC during aging (**Fig. 6a**).

The remodeling of EC and MSC interactions highlights the vascular weakening observed in the BM with aging. Specifically, delta-like ligand 4 (*DLL4*), a Notch ligand crucial for angiogenesis[61], interacted with *NOTCH1-4* in young EC and MSC. In contrast, in aged EC, *DLL4* interactions were replaced by *JAG1,* indicating impaired blood vessel formation (**Fig. 6b**). This observation was further supported by age-related vascular endothelial growth factor (VEGF) family alterations. In young BM, *VEGFA* mediated interactions with endothelial receptors *KDR*, *FLT1, NRP1,* and *NRP2*, whereas *VEGFB* was predominant in aged individuals (**Fig. 6b**). Additionally, interactions mediated by *GDF7* and bone morphogenetic protein (BMP) elements, presented in the young stroma, were notably absent in aged cells (**Fig. 6b**). Interestingly, the altered EC-MSC communication in the aged BM was consisted with the age-related shift in MSC differentiation towards adipocytes at the expense of osteoblast differentiation. The aged BM microenvironment exhibited a more adipogenic phenotype as evidenced by the interactions involving apolipoproteins (*APOB* and *APOE* with *LDLR* in MSC and *APOD* from EC with *LEPR* in MSC) (**Fig. 6b**).

A more detailed analysis of the interactions between the RAB13^{+} arterial-like EC and the THY1^{+}Fibro-MSC populations identified specific L–R pairs that became more prominent in the aged BM (**Fig. 6c**). Notably, interactions like *SLIT2-ROBO4*, *SLIT3-ROBO4,* and *SFRP1-FZD6* were exclusive to aged individuals. Interestingly, the expression of *SRFP1* and *FZD6* has been described to increase in aged senescent cells, suggesting their potential as markers for targeting Wnt signaling and senescence-related aging in the BM[62,63]. Additionally, aged THY1^{+}Fibro-MSC exhibited extensive crosstalk with both EC and MSC subpopulations through *SDC2* receptor interactions, implicating cell adhesion and ECM processes in the aging BM microenvironment (**Fig. 6d**).

Overall, our findings highlight key L-R interactions that may contribute to communication changes potentially driving senescence and profibrotic rewiring of aged BM cells, uncovering key molecular pathways involved in BM aging.

Impact of aging on the BM microenvironment interactome
Our next cell-cell interaction analysis investigated the interactions between EC, MSC, and the broader BM microenvironment during aging (**Extended Data Fig. 8a-b**). Interestingly, interactions with DC increased with age, possibly influenced by the chronic inflammation commonly observed in elderly individuals[64] (**Fig. 6e**). By examining the age-related changes on specific ligands and receptors, *FN1* appeared as a pivotal interactor of the aged BM microenvironment (**Fig. 6f**). *FN1* ligand primarily expressed by MSC, DC, and mainly EC interacts with different members of the integrins family further implicating ECM remodeling along the aging process. The increased *FN1* communication observed in aged EC may reflect a remodeling of the basement membrane, potentially contributing to EC activation[65]. Furthermore, the transforming growth factor-beta 1 (*TGFB1*) predicted interactions in aged EC and MSC increased in comparison with young BM (**Extended Data Fig. 8c**). The interactions of *TGFB1* with their receptors and several integrins, such as *ITGAV* on MSC, which were specific to the aged BM microenvironment, suggest its role in driving age-related fibrosis.

The elevated inflammatory cytokine signaling aligns with the pro-inflammatory state described in the aged BM (**Fig. 6g**). *CXCL12*, a key mediator in aged EC, interacted through *CXCR4* and *ITGB1* across ProB cells, platelets, DC, and CD8-NK like T cells. *CXCL12* from aged EC also

interacted with EC, MSC, and DC through *CD4*. Additionally, *ACKR1* from EC and erythroblasts interacted with various hematopoietic cell types via CXCL family members (*CXCL8*, *CXCL2*, *CXCL1*) and CCL chemokines (*CCL14*), all of which are known to play a role in inflammation[66]. This shift toward a pro-inflammatory state with aging was further accentuated by the increased interactions mediated through *MIF*, *CD74*, and *CD99* ligands in the aged BM microenvironment (**Extended Data Fig. 8d**).

In conclusion, the remodeling of the BM microenvironment interactome during aging suggests the role of non-hematopoietic components, particularly through increased communication with DC, in shaping the pro-inflammatory milieu observed in the BM of aged individuals. Importantly, the *FN1* and *TGFB1* pathways may represent potential therapeutic targets for mitigating fibrotic processes in the aging BM.

Spatial transcriptomics uncovers vascular alterations along the aging process

We have characterized the age-related shifts in BM non-hematopoietic cell proportions, molecular profiles, and cell-to-cell communication. However, the spatial molecular configuration within this context remains largely unexplored. To address this gap, we employed spatial transcriptomics using FFPE BM from two new samples, one young (34 years of age) and one elderly (76 years of age), using the Visium Gene Expression platform (10X Genomics)[67] (**Supplementary Table 2**). After pre-processing and quality control analysis, we detected 757 and 810 spots in young and elderly samples, respectively, with an average of 612 features and 1417 counts per spot in the young and 561 features and 1415 counts in the elderly (data not shown).

Given our interest in characterizing aging-related shifts in EC and MSC, we first aimed to identify the spots with a higher likelihood of containing specific cell types. To label the spots, we used a scRNA-seq atlas generated by Bandyopadhyay et al.[25] as a reference and conducted an annotation analysis. First, we estimated both cell proportion and a signature score per cell type per spot (**Extended Data Fig. 9a-c**). Then, for each cell type, spots highly ranked for both measures were considered "high-confidence spots" for such cell type as detailed in supplemental methods (**Extended Data Fig. 9d-f and data not shown**). All the analyses were conducted separately for both samples, resulting in a subset of spots highly enriched for each cell type, mapping EC, MSC, as well as hematopoietic cells, including HSC, B cells, DC, erythroblasts, monocytes, neutrophils, PC, and T cells in the human BM (**Fig. 7a and data not shown)**. The spatial enrichment of endothelial and stromal cell populations was further validated using IF and Hematoxylin-Eosin (H&E) staining (**Fig. 7b and Extended Data Fig. 9g**). Specifically, non-hematopoietic niche cells were localized around blood vessels and identified by IF using colocalization of specific markers EC ($CD31^+$ $CD45^-$) and MSC ($PRRX1^+$ $CD45^-$).

Next, we explored the spatial expression patterns of age-related transcriptional changes observed in our scRNA-seq analysis, focusing on EC. Even though we lack sufficient statistical power, we observed higher values of the RAB13-related signature in aged EC spots, providing additional evidence that the $RAB13^+$ EC state could significantly influence the aging process within the human BM (**Fig. 7c-d**). Notably, RAB13-related cells colocalized with the spatial expression pattern of *YBX1*, a key TF involved in RNA splicing and translation control upregulated in $RAB13^+$ cells (**Extended Data Fig. 10a)**. Aged EC also displayed an increased tendency for senescence pathway further resembling the characteristics of $RAB13^+$ EC (**Extended Data Fig. 10b**). The spatial enrichment of this EC subset with aging was further confirmed through IF staining of $RAB13^+$ cells from FFPE BM biopsies (**Fig. 7e**). $RAB13^+$ EC were more abundant in the aged BM validating our previous transcriptomic findings. It is noteworthy that RAB13 expression was predominantly localized near the periarteriolar regions, as evidenced by the proximity of $RAB13^+$ $CD31^+$ EC to α-$SMA1^+$ cells (**Fig. 7e**).

Consistent with the significant age-related increase in the venous cluster and supporting the "inflammation and immune" hypothesis, we found elevated spatial expression of *CLU* and *CD74* in aged EC (**Extended Data Fig. 10c**). Additionally, aged EC-labeled spots displayed a marked

shift towards oxidative metabolism, which aligns with the mitochondrial dysfunction identified in aged sinusoids through our scRNA-seq analysis (**Extended Data Fig. 10d**). Furthermore, *VIM* and *GSN*, two genes implicated in ECM regulation and previously found upregulated in aged sinusoids, were highly expressed in aged EC (**Extended Data Fig. 10e**). These findings highlight *VIM* and *GSN* as potential biomarkers of endothelial aging.

Finally, spatial resolution analysis of L-R interactions corroborated several findings from our previous BM microenvironment cell-to-cell communication analysis. Specifically, we observed reduced *BMPR2* expression in spots enriched in aged EC, indicating diminished support for osteogenic differentiation through EC-MSC interactions in the aged BM (**Extended Data Fig. 10f-g)**. Conversely, *JAG1-NOTCH3* signaling was detected in spots enriched in aged EC, suggesting a shift in BM cell communication dynamics with aging (**Fig. 7f)**. In line with the increased interactions between niche cells and DC identified by our scRNA-seq analysis, EC-labeled spots in aged BM showed a significant positive correlation with the DC score, further implicating EC-DC communication in shaping the pro-inflammatory milieu observed in the aged BM (**Extended Data Fig. 10h)**. Interestingly, we discerned elevated spatial expression of the *FN1* ligand in spots enriched in aged EC, corroborating the observed ECM remodeling detected in our previous transcriptomic data (**Fig. 7g and Extended Data Fig. 10i)**. This last result emphasizes FN1 as a key interactor driving ECM changes in the aged BM microenvironment.

Our findings uncover spatially distinct, age-related changes within the human non-hematopoietic BM microenvironment, with a notable impact on EC. Supported by our scRNA-seq analysis, these results underscore key alterations in cell state distribution, signaling pathways, and intercellular communication within the aged BM.

DISCUSSION

In recent decades, our understanding of how the human BM ages has advanced significantly, with scRNA-seq technologies providing deep insights into the heterogeneity and mechanistic evolution of HSC during aging[68–72]. In addition, the investigation of the aged HSC niche revealed many unanticipated changes in the BM microenvironment that contribute to the decline in HSC function over time[10,73–75]. These insights positioned the BM microenvironment as a potential target for rejuvenation. However, due to the limitations of studying human aging, most studies have relied on mouse models[11,76,77].

Here, we provide a comprehensive transcriptional characterization of the changes that occur during physiological aging of the BM non-hematopoietic microenvironment with a special focus on endothelial and mesenchymal compartments. Additionally, using IF staining and spatial transcriptomic profiling, we provide valuable initial insights into the spatial organization of these cells, but most significantly, we provide support for some of the findings derived from the scRNA-seq analysis of BM aging.

Our findings expand on the well-characterized arteries sinusoids[25] and uncovered previously undescribed vascular subtypes within the human BM endothelium, including capillaries and venous. Importantly, we revealed significant age-dependent shifts in EC cluster distribution, notably an increased prevalence of the venous cluster in elderly samples, marked by genes related to immune activation and coagulation. This indicates a shift towards enhanced inflammation and elevated thrombotic activity with aging in EC. Interestingly, we discovered an arterial-related cluster in aged EC, characterized by the high expression of *RAB13* associated with dysregulation of transcriptional elongation activity and cellular senescence process. The spatial enrichment of this arterial-associated EC subset during aging was further demonstrated by IF staining, showing colocalization of RAB13^{+} cells with CD31^{+} EC and α-SMA1^{+} cells. This newly identified aging-related subset, revealed through scRNA-seq and spatial transcriptomics, is regulated by the TF ZEB1[40,78] and demonstrated elevated expression of RBP, positioning these cells as candidate regulators of aging and promoters of cellular senescence[37,79,80]. The role of RAB13 in cancer progression is well-documented, making the identification of RAB13^{+} cells as a novel subset of

aged EC a potential therapeutic target[63]. Sinusoids were identified as the most distinct vascular bed during aging, exhibiting a prothrombotic profile, mitochondrial dysfunction, and a decline in transcriptional activity. Moreover, they have been described as major contributors to endothelial senescence[81]. Aged sinusoids also showed a signature associated with an impaired ability to maintain vascular integrity and angiogenic potential, possibly promoting a regression in the vasculature structure and disrupting inflammatory homeostasis, consistent with previous studies conducted in mice[8,14,76].

Despite considerable advancements in characterizing the human BM stroma, age-related transcriptional changes in MSC remain unresolved[23,25,82,83]. Notably, our results revealed the emergence of THY1$^+$Fibro-MSC in the aged stroma, which exhibited high similarity to the recently identified THY1$^+$MSC subpopulation[25]. These cells showed an enrichment of genes associated with TGF-β signaling pathway, ECM organization, and EMT, suggesting the implication of these profibrotic processes in aged MSC. We also confirmed histologically that CD90$^+$ BM MSC coexist with fibrosis[84,85]. Furthermore, analyzing the transcriptional changes along MSC aging showed an increase of ATP metabolism and OXPHOS in aged individuals, reduced UPR, and impaired support for hematopoietic and osteoblast differentiation[86–89]. Overall, our findings reveal extensive transcriptional remodeling within the endothelial and mesenchymal compartments of the BM, characterized by increased inflammation, impaired mitochondrial and ribosomal function, and elevated ROS production. These age-specific changes align with established hallmarks of aging[90,91], positioning EC and MSC as promising targets for strategies aimed at rejuvenating the aged BM microenvironment[87,92].

The differences in the BM microenvironment significantly influence the behavior and regenerative capacity of aged HSC[93]. Therefore, studying this crosstalk is vital for developing therapeutic strategies to mitigate age-related decline in HSC function and improve health outcomes in older people. The shift from *VEGFA* to *VEGFB* interactions and the altered NOTCH signaling observed in aged EC may contribute to impaired blood vessel formation during aging[94,95]. This disruption of NOTCH signaling supports previous studies highlighting its role in maintaining HSC stemness[12,14]. Moreover, the aged BM niche showed increased apolipoprotein interactions, consistent with the accumulation of adipocytes during BM aging and the compromised differentiation of aged MSC[18]. Remarkably, we identified *SFRP1-FZD6* and *SDC2* receptor interactions as potential key regulators of senescence and ECM processes related to the emergence of RAB13$^+$ EC state and THY1$^+$Fibro-MSC population during aging. *FN1* and *TGFB1* emerged as central signaling hubs in the aged BM microenvironment, reflecting impaired matrix remodeling and potentially driving cell activation and inflammatory processes[18,65]. This shift toward a pro-inflammatory state during the aging process was reinforced by the enhanced communication with DC and the increased interactions mediated by cytokine signaling, *MIF*, *CD74*, and *CD99*.

Despite the technical limitations associated with applying spatial transcriptomics to mineralized tissues and BM in particular [28,96,97], we could perform Visium Gene Expression technology from 10X Genomics on human FFPE BM biopsies from young and elderly individuals. We comprehensively detailed the spatial organization of the human BM by meticulously mapping the distribution of the hematopoietic and non-hematopoietic components within the BM niche. This was validated by expressing CD45, CD31, and PRRX1 using IF. Importantly, we spatially validated the EC alterations previously identified in our scRNA-seq data. Notably, we detected an increased spatial localization of RAB13$^+$ senescent cells near periarteriolar regions, alongside distal EC showing elevated expression of *GSN* in the aged BM. Additionally, our spatial transcriptomic data confirmed the enhanced communication of aged EC with DC and the FN1 signaling pathway as a central interaction hub in the aged BM.

In summary, our study provides novel insights into the age-related remodeling of the EC and MSC transcriptome, interactome, and spatial architecture, offering potential explanations for the hematopoietic system deterioration observed during aging. We find that aging compromises the

ability of EC to maintain vascular integrity and reduces the protein folding capacity and support for hematopoietic differentiation of MSC. Both cell types exhibit compromised mitochondrial function and heightened inflammatory and prothrombotic properties with age. We also identified an aged-related EC subset responsible for translation and senescence processes. Moreover, we observe a more fibrotic and less functional aged BM stroma influenced by THY1^{+}Fibro-MSC, which may contribute to its diminished capacity to support hematopoiesis in aging-related pathologies. Our spatial transcriptomics analysis suggests a significant spatial disorganization of endosteal and vascular structures. This analysis also confirms our previous scRNA-seq results, highlighting the presence of RAB13^{+} senescent cells in aged EC and age-associated interactions. Collectively, our results emphasize the critical role of non-hematopoietic components in shaping the functional trajectory and longevity of HSC. These age-related alterations position the non-hematopoietic BM niche as a promising therapeutic target for mitigating hematopoietic decline and enhancing tissue regeneration in aging populations.

ACKNOWLEDGEMENTS
This work was supported by the Instituto de Salud Carlos III and co-financed by ERDF A way of making Europe (PI20/01308, PI23/00516); CIBERONC (CB16/12/00489), RICORS TERAV (RD21/0017/0009); Departamento de Industria Gobierno de Navarra (AGATA 0011-1411-2020-000010/0011-1411-2020-000011) and Departamento de Salud Gobierno de Navarra to F.P.. The study was also supported by The Spanish Government through project PID2019-111192GA-I00 (MICINN) to D.G.C.. I.A.C. was supported by a Marie Curie grant (H2020- MSCA-IF-837491) from the European Commission. I.C. was endorsed by an AECC predoctoral fellowship (PRDNA19006CENZ). M.C. was supported by an FPU fellowship (FPU22/03283) from Ministerio de Ciencia, Innovación y Universidades.

We would like to thank the staff of the flow cytometry core and the advanced genomic lab for their invaluable technical and intellectual assistance. We also acknowledge Hospital Universitario de Navarra and Hospital Reina Sofía de Tudela for providing the human BM samples and their collaboration. We are particularly grateful to the healthy donors for participating in this study.

AUTHORSHIP CONTRIBUTIONS
I.A.C., I.C. and M.C. processed human BM samples. I.C. analyzed the scRNA-seq data and performed the cell-to-cell interactome. A.R.L.P. analyzed the spatial transcriptomic data. J.R., I.S.G., M.M.B., and D.Q.A. provided the BM samples. P.S.M., P.A.R., and A.V. performed the scRNA-seq experiments. D.A. and A.L. performed the FACS sorting. I.A.C., I.C., and M.C. interpreted the data and wrote the paper. S.S., P.R.C., P.S.M., and P.A.R. performed the spatial transcriptomic experiments. M.C., and L.C-D. performed the histologic analysis. D.G.C., with help from J.Y., L.S., R.L., and J.T., supervised the computational work. M.A-M. and E.M. contributed by providing the myelofibrosis samples. I.A.C. and B.S. conceptualized the study. F.P., D.G.C., and I.A.C conceived and directed the research project. All authors actively participated in the discussions underlying this manuscript. F.P., D.G.C., I.A.C, I.C., and M.C. discussed the results and wrote the final manuscript. All authors contributed to, read, and approved the final manuscript.

DISCLOSURE OF CONFLICTS OF INTEREST
The authors declare no competing interests.

REFERENCES

1. Eaves, C. J. Hematopoietic stem cells: Concepts, definitions, and the new reality. *Blood* **125**, 2605–2613 (2015).
2. Schofield, R. The relationship between the spleen colony-forming cell and the haemopoietic stem cell. *Blood Cells* **4**, 7–25 (1978).
3. Morrison, S. J. & Scadden, D. T. The bone marrow niche for haematopoietic stem cells. *Nature* **505**, 327–334 (2014).
4. Pinho, S. & Frenette, P. S. Haematopoietic stem cell activity and interactions with the niche. *Nat Rev Mol Cell Biol* **20**, 303–320 (2019).
5. Fröbel, J. *et al.* The Hematopoietic Bone Marrow Niche Ecosystem. *Front Cell Dev Biol* **9**, (2021).
6. Khan, S. S., Singer, B. D. & Vaughan, D. E. Molecular and physiological manifestations and measurement of aging in humans. *Aging Cell* **16**, 624–633 (2017).
7. Chen, Q. *et al.* Fate decision of mesenchymal stem cells: adipocytes or osteoblasts? *Cell Death & Differentiation 2016 23:7* **23**, 1128–1139 (2016).
8. Winter, S. *et al.* Clonal hematopoiesis and its impact on the aging osteo-hematopoietic niche. *Leukemia 2024 38:5* **38**, 936–946 (2024).
9. Guo, J. *et al.* Aging and aging-related diseases: from molecular mechanisms to interventions and treatments. *Signal Transduct Target Ther* **7**, 391 (2022).
10. López-Otín, C., Blasco, M. A., Partridge, L., Serrano, M. & Kroemer, G. Hallmarks of aging: An expanding universe. *Cell* **186**, 243–278 (2023).
11. Ramalingam, P. *et al.* Restoring bone marrow niche function rejuvenates aged hematopoietic stem cells by reactivating the DNA Damage Response. *Nature Communications 2023 14:1* **14**, 1–20 (2023).
12. Kusumbe, A. P. *et al.* Age-dependent modulation of vascular niches for haematopoietic stem cells. *Nature* **532**, 380–384 (2016).
13. Poulos, M. G. *et al.* Endothelial transplantation rejuvenates aged hematopoietic stem cell function. *Journal of Clinical Investigation* **127**, 4163–4178 (2017).
14. Ho, Y.-H. & Méndez-Ferrer, S. Microenvironmental contributions to hematopoietic stem cell aging. *Haematologica* **105**, 38–46 (2020).
15. Dobner, S., Tóth, F. & de Rooij, L. P. M. H. A high-resolution view of the heterogeneous aging endothelium. *Angiogenesis 2024 27:2* **27**, 129–145 (2024).
16. Boueya, I. L., Sandhow, L., Albuquerque, J. R. P., Znaidi, R. & Passaro, D. Endothelial heterogeneity in bone marrow: insights across development, adult life and leukemia. *Leukemia 2024* 1–17 (2024) doi:10.1038/s41375-024-02453-x.
17. Kusumbe, A. P. *et al.* Age-dependent modulation of vascular niches for haematopoietic stem cells. *Nature* **532**, 380–384 (2016).
18. Al-Azab, M., Safi, M., Idiiatullina, E., Al-Shaebi, F. & Zaky, M. Y. Aging of mesenchymal stem cell: machinery, markers, and strategies of fighting. *Cellular & Molecular Biology Letters 2022 27:1* **27**, 1–40 (2022).
19. Helbling, P. M. *et al.* Global Transcriptomic Profiling of the Bone Marrow Stromal Microenvironment during Postnatal Development, Aging, and Inflammation. *Cell Rep* **29**, 3313-3330.e4 (2019).
20. Chen, W. *et al.* A global view of altered ligand-receptor interactions in bone marrow aging based on single-cell sequencing. *Comput Struct Biotechnol J* **23**, 2754–2762 (2024).
21. Wang, Z. *et al.* Single-cell RNA sequencing deconvolutes the in vivo heterogeneity of human bone marrow-derived mesenchymal stem cells. *Ivyspring International Publisher Int. J. Biol. Sci* **2021**, 4192–4206 (2021).

22. Ye, J. *et al.* Deconvolution of the hematopoietic stem cell microenvironment reveals a high degree of specialization and conservation. *iScience* **25**, (2022).
23. Li, H. *et al.* Identification of phenotypically, functionally, and anatomically distinct stromal niche populations in human bone marrow based on single-cell RNA sequencing. *Elife* **12**, (2023).
24. Fiévet, L. *et al.* Single-cell RNA sequencing of human non-hematopoietic bone marrow cells reveals a unique set of inter-species conserved biomarkers for native mesenchymal stromal cells. *Stem Cell Res Ther* **14**, 1–16 (2023).
25. Bandyopadhyay, S. *et al.* Mapping the cellular biogeography of human bone marrow niches using single-cell transcriptomics and proteomic imaging. *Cell* **187**, 3120-3140.e29 (2024).
26. Cenzano, I. *et al.* Transcriptional Remodeling of the Stromal and Endothelial Microenvironment in MGUS to Multiple Myeloma Progression. *bioRxiv* 2024.04.24.589777 (2024) doi:10.1101/2024.04.24.589777.
27. Stuart, T. *et al.* Comprehensive Integration of Single-Cell Data. *Cell* **177**, 1888-1902.e21 (2019).
28. Sudupe, L. *et al.* Spatial Transcriptomics Reveals a Myeloma Cell Architecture with Dysfunctional T-Cell Distribution, Neutrophil Traps, and Inflammatory Signaling. *bioRxiv* 2024.07.03.601833 (2024) doi:10.1101/2024.07.03.601833.
29. Ma, Y. & Zhou, X. Spatially informed cell-type deconvolution for spatial transcriptomics. *Nature Biotechnology 2022 40:9* **40**, 1349–1359 (2022).
30. Kalucka, J. *et al.* Single-cell transcriptome atlas of murine endothelial cells. *Cell* **180**, 764-779.e20 (2020).
31. Thiriot, A. *et al.* Differential DARC/ACKR1 expression distinguishes venular from non-venular endothelial cells in murine tissues. *BMC Biol* **15**, 1–19 (2017).
32. Ashburner, M. *et al.* Gene Ontology: tool for the unification of biology. *Nature Genetics 2000 25:1* **25**, 25–29 (2000).
33. Consortium, T. G. O. *et al.* The Gene Ontology knowledgebase in 2023. *Genetics* **224**, (2023).
34. Hopkin, S., Lord, J. M. & Chimen, M. Dysregulation of leukocyte trafficking in ageing: Causal factors and possible corrective therapies. *Pharmacol Res* **163**, 105323 (2021).
35. Wechter, N. *et al.* Single-cell transcriptomic analysis uncovers diverse and dynamic senescent cell populations. *Aging (Albany NY)* **15**, 2824 (2023).
36. Ximerakis, M. *et al.* Single-cell transcriptomic profiling of the aging mouse brain. *Nature Neuroscience 2019 22:10* **22**, 1696–1708 (2019).
37. Varesi, A. *et al.* RNA binding proteins in senescence: A potential common linker for age-related diseases? *Ageing Res Rev* **88**, (2023).
38. Aibar, S. *et al.* SCENIC: Single-cell regulatory network inference and clustering. *Nat Methods* **14**, 1083 (2017).
39. Almotiri, A. *et al.* Zeb1 maintains long-term adult hematopoietic stem cell function and extramedullary hematopoiesis. *Exp Hematol* **134**, (2024).
40. Yu, Q. C. *et al.* Activation of Wnt/β-catenin signaling by Zeb1 in endothelial progenitors induces vascular quiescence entry. *Cell Rep* **41**, (2022).
41. Siles, L., Ninfali, C., Cortés, M., Darling, D. S. & Postigo, A. ZEB1 protects skeletal muscle from damage and is required for its regeneration. *Nat Commun* **10**, (2019).
42. Stucker, S., Chen, J., Watt, F. E. & Kusumbe, A. P. Bone Angiogenesis and Vascular Niche Remodeling in Stress, Aging, and Diseases. *Front Cell Dev Biol* **8**, 602269 (2020).

43. Sepúlveda, C., Palomo, I. & Fuentes, E. Mechanisms of endothelial dysfunction during aging: Predisposition to thrombosis. *Mech Ageing Dev* **164**, 91–99 (2017).
44. Akrivou, D., Perlepe, G., Kirgou, P., Gourgoulianis, K. I. & Malli, F. Pathophysiological Aspects of Aging in Venous Thromboembolism: An Update. *Medicina (Kaunas)* **58**, (2022).
45. Chen, M. B., Yang, A. C., Lehallier, B., Quake, S. R. & Wyss-Coray, T. Brain Endothelial Cells Are Exquisite Sensors of Age-Related Circulatory Cues. (2020) doi:10.1016/j.celrep.2020.03.012.
46. Zhang, M. J., Pisco, A. O., Darmanis, S. & Zou, J. Mouse aging cell atlas analysis reveals global and cell type-specific aging signatures. *Elife* **10**, (2021).
47. Tian, Y. *et al.* Iron Metabolism in Aging and Age-Related Diseases. *Int J Mol Sci* **23**, 3612 (2022).
48. Churchman, S. M. *et al.* Transcriptional profile of native CD271+ multipotential stromal cells: Evidence for multiple fates, with prominent osteogenic and wnt pathway signaling activity. *Arthritis Rheum* **64**, 2632–2643 (2012).
49. Baryawno, N. *et al.* A Cellular Taxonomy of the Bone Marrow Stroma in Homeostasis and Leukemia. *Cell* **177**, 1915-1932.e16 (2019).
50. Sanchez-Niño, M. D. *et al.* MIF, CD74 and other partners in kidney disease: tales of a promiscuous couple. *Cytokine Growth Factor Rev* **24**, 23–40 (2013).
51. Xia, P. *et al.* Therapeutic effects of recombinant human S100A6 and soluble receptor for advanced glycation end products(sRAGE) on CCl4-induced liver fibrosis in mice. *Eur J Pharmacol* **833**, 86–93 (2018).
52. Wu, X. *et al.* Regulating the cell shift of endothelial cell-like myofibroblasts in pulmonary fibrosis. *European Respiratory Journal* **61**, (2023).
53. Agarwal, A. *et al.* Bone marrow fibrosis in primary myelofibrosis: pathogenic mechanisms and the role of TGF-β. *Stem Cell Investig* **3**, (2016).
54. Ghosh, K., Shome, D. K., Kulkarni, B., Ghosh, M. K. & Ghosh, K. Fibrosis and bone marrow: understanding causation and pathobiology. *J Transl Med* **21**, 703 (2023).
55. Longhitano, L. *et al.* IGFBP-6/sonic hedgehog/TLR4 signalling axis drives bone marrow fibrotic transformation in primary myelofibrosis. *Aging (Albany NY)* **13**, 25055 (2021).
56. Meessen, J. M. T. A. *et al.* IGFBP7 and GDF-15, but not P1NP, are associated with cardiac alterations and 10-year outcome in an elderly community-based study. *BMC Cardiovasc Disord* **21**, (2021).
57. Al-Azab, M., Safi, M., Idiiatullina, E., Al-Shaebi, F. & Zaky, M. Y. Aging of mesenchymal stem cell: machinery, markers, and strategies of fighting. *Cell Mol Biol Lett* **27**, 69 (2022).
58. Duscher, D. *et al.* Aging disrupts cell subpopulation dynamics and diminishes the function of mesenchymal stem cells. doi:10.1038/srep07144.
59. Zhang, Y. *et al.* Adult mesenchymal stem cell ageing interplays with depressed mitochondrial Ndufs6. *Cell Death Dis* **11**, 1075 (2020).
60. Ghosh, D. *et al.* Senescent mesenchymal stem cells remodel extracellular matrix driving breast cancer cells to more invasive phenotype. *J Cell Sci* (2020) doi:10.1242/jcs.232470.
61. Akil, A. *et al.* Notch Signaling in Vascular Endothelial Cells, Angiogenesis, and Tumor Progression: An Update and Prospective. *Front Cell Dev Biol* **9**, 642352 (2021).

62. Brunt, K. R. *et al.* Role of WNT/β-Catenin Signaling in Rejuvenating Myogenic Differentiation of Aged Mesenchymal Stem Cells from Cardiac Patients. *Am J Pathol* **181**, 2067–2078 (2012).
63. Donega, V. *et al.* Single-cell profiling of human subventricular zone progenitors identifies SFRP1 as a target to re-activate progenitors. *Nature Communications 2022 13:1* **13**, 1–12 (2022).
64. Agrawal, A., Agrawal, S. & Gupta, S. Role of Dendritic Cells in Inflammation and Loss of Tolerance in the Elderly. *Front Immunol* **8**, (2017).
65. Al-Yafeai, Z. *et al.* Endothelial FN (Fibronectin) deposition by α5β1 integrins drives atherogenic inflammation. *Arterioscler Thromb Vasc Biol* **38**, 2601–2614 (2018).
66. Do, H. T. T., Lee, C. H. & Cho, J. Chemokines and their Receptors: Multifaceted Roles in Cancer Progression and Potential Value as Cancer Prognostic Markers. *Cancers (Basel)* **12**, (2020).
67. Ståhl, P. L. *et al.* Visualization and analysis of gene expression in tissue sections by spatial transcriptomics. *Science (1979)* **353**, 78–82 (2016).
68. Gao, S. *et al.* Comparative transcriptomic analysis of the hematopoietic system between human and mouse by single cell rna sequencing. *Cells* **10**, 973 (2021).
69. Anjos-Afonso, F. *et al.* Single cell analyses identify a highly regenerative and homogenous human CD34+ hematopoietic stem cell population. *Nature Communications 2022 13:1* **13**, 1–13 (2022).
70. Calvanese, V. *et al.* Mapping human haematopoietic stem cells from haemogenic endothelium to birth. *Nature 2022 604:7906* **604**, 534–540 (2022).
71. Weng, C. *et al.* Deciphering cell states and genealogies of human haematopoiesis. *Nature 2024 627:8003* **627**, 389–398 (2024).
72. Quaranta, P. *et al.* Circulating hematopoietic stem/progenitor cell subsets contribute to human hematopoietic homeostasis. *Blood* **143**, 1937–1952 (2024).
73. Guidi, N. *et al.* An aged bone marrow niche restrains rejuvenated hematopoietic stem cells. *Stem Cells* **39**, 1101–1106 (2021).
74. Kwon, M., Kim, B. S., Yoon, S., Oh, S. O. & Lee, D. Hematopoietic Stem Cells and Their Niche in Bone Marrow. *International Journal of Molecular Sciences 2024, Vol. 25, Page 6837* **25**, 6837 (2024).
75. Feng, C., Fan, H., Tie, R., Xin, S. & Chen, M. Deciphering the evolving niche interactome of human hematopoietic stem cells from ontogeny to aging. *Front Mol Biosci* **11**, (2024).
76. Ho, Y. H. *et al.* Remodeling of Bone Marrow Hematopoietic Stem Cell Niches Promotes Myeloid Cell Expansion during Premature or Physiological Aging. *Cell Stem Cell* **25**, 407-418.e6 (2019).
77. Yuan, N. *et al.* Young donor hematopoietic stem cells revitalize aged or damaged bone marrow niche by transdifferentiating into functional niche cells. *Aging Cell* **22**, (2023).
78. Schwab, A. *et al.* Zeb1 mediates EMT/plasticity-associated ferroptosis sensitivity in cancer cells by regulating lipogenic enzyme expression and phospholipid composition. *Nature Cell Biology 2024* 1–12 (2024) doi:10.1038/s41556-024-01464-1.
79. Han, Y. & Kim, S. Y. Endothelial senescence in vascular diseases: current understanding and future opportunities in senotherapeutics. *Experimental & Molecular Medicine 2022 55:1* **55**, 1–12 (2023).

80. Kalies, K. *et al.* Isolation of circulating endothelial cells provides tool to determine endothelial cell senescence in blood samples. *Scientific Reports 2024 14:1* **14**, 1–13 (2024).
81. Luo, Z., Yao, J., Wang, Z. & Xu, J. Mitochondria in endothelial cells angiogenesis and function: current understanding and future perspectives. *J Transl Med* **21**, (2023).
82. de Jong, M. M. E. *et al.* The multiple myeloma microenvironment is defined by an inflammatory stromal cell landscape. *Nature Immunology 2021 22:6* **22**, 769–780 (2021).
83. Gao, Y. *et al.* Multi-omics analysis of human mesenchymal stem cells shows cell aging that alters immunomodulatory activity through the downregulation of PD-L1. *Nat Commun* **14**, (2023).
84. Decker, M. *et al.* Leptin-receptor-expressing bone marrow stromal cells are myofibroblasts in primary myelofibrosis. *Nature Cell Biology 2017 19:6* **19**, 677–688 (2017).
85. Dudli, S. *et al.* CD90-positive stromal cells associate with inflammatory and fibrotic changes in modic changes. *Osteoarthr Cartil Open* **4**, (2022).
86. Fraile, M., Eiro, N., Costa, L. A., Martín, A. & Vizoso, F. J. Aging and Mesenchymal Stem Cells: Basic Concepts, Challenges and Strategies. *Biology 2022, Vol. 11, Page 1678* **11**, 1678 (2022).
87. Barilani, M. *et al.* Age-related changes in the energy of human mesenchymal stem cells. *J Cell Physiol* **237**, 1753–1767 (2022).
88. Tavasolian, F. *et al.* Unfolded protein response-mediated modulation of mesenchymal stem cells. *IUBMB Life* **72**, 187–197 (2020).
89. Zhang, H. *et al.* The roles of bone remodeling in normal hematopoiesis and age-related hematological malignancies. *Bone Res* **11**, (2023).
90. Yang, X. *et al.* Aged mesenchymal stem cells and inflammation: from pathology to potential therapeutic strategies. *Biol Direct* **18**, 1–12 (2023).
91. Maldonado, E., Morales-Pison, S., Urbina, F. & Solari, A. Aging Hallmarks and the Role of Oxidative Stress. *Antioxidants 2023, Vol. 12, Page 651* **12**, 651 (2023).
92. Mistry, J. J. *et al.* Mesenchymal Stromal Cell Senescence Induced by Dnmt3a-Mutant Hematopoietic Cells is a Targetable Mechanism Driving Clonal Hematopoiesis and Initiation of Hematologic Malignancy. *bioRxiv* 2024.03.28.587254 (2024) doi:10.1101/2024.03.28.587254.
93. How age affects human hematopoietic stem and progenitor cells and the strategies to mitigate aging. *Exp Hematol* **143**, 104711 (2025).
94. Seto, M. *et al.* Multi-omic characterization of brain changes in the vascular endothelial growth factor family during aging and Alzheimer's disease. *Neurobiol Aging* **126**, 25–33 (2023).
95. Rastogi, C. *et al.* Counteracting age-related VEGF signaling insufficiency promotes healthy aging and extends life span. *Science (1979)* **373**, E3692–E3701 (2021).
96. Singh, V. M. *et al.* Analysis of the effect of various decalcification agents on the quantity and quality of nucleic acid (DNA and RNA) recovered from bone biopsies. *Ann Diagn Pathol* **17**, 322–326 (2013).
97. Xiao, X. *et al.* Spatial transcriptomic interrogation of the murine bone marrow signaling landscape. *Bone Research 2023 11:1* **11**, 1–13 (2023).

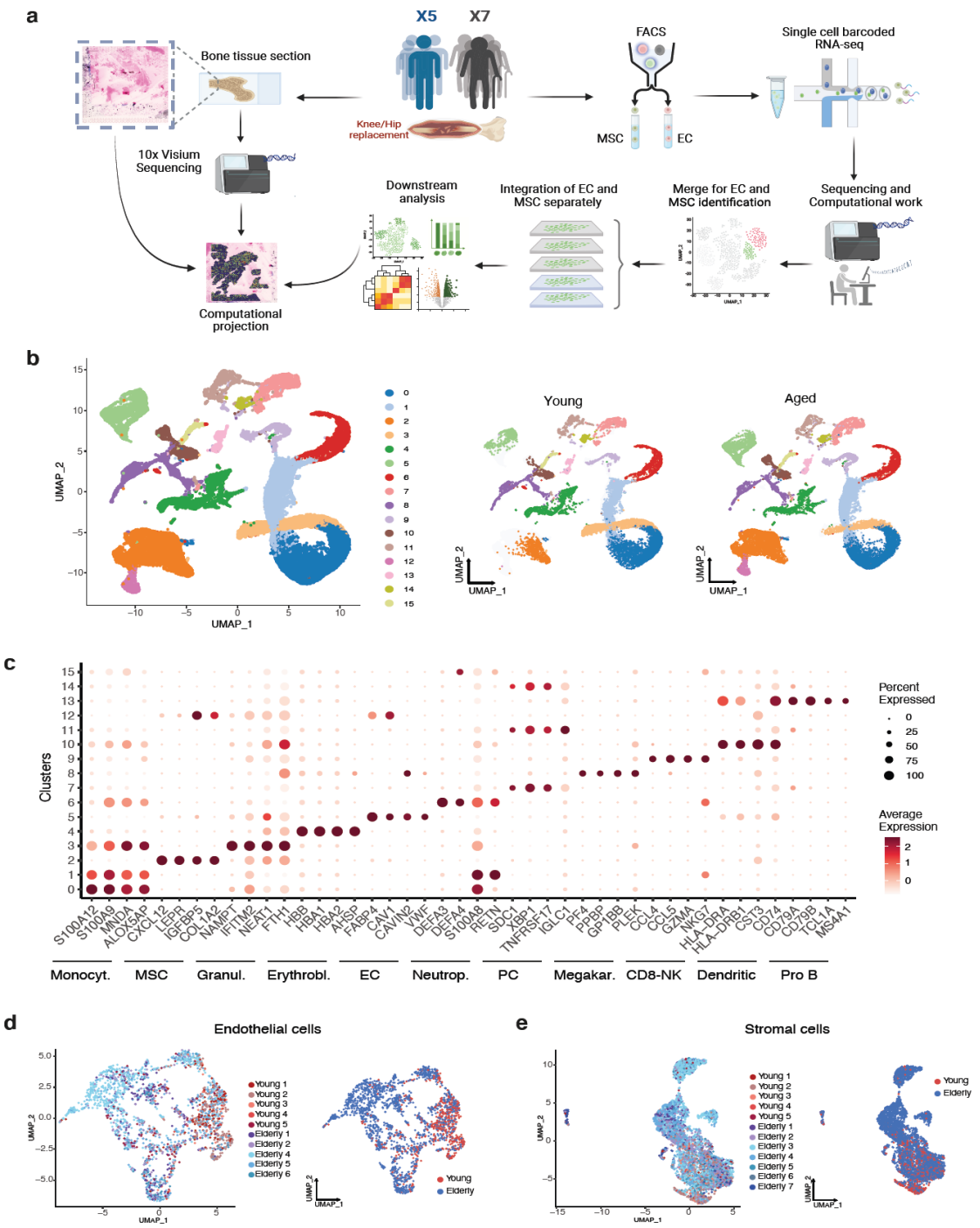

Figure 1. Transcriptional profiling of human young and aged BM endothelial and stromal cells.
a. Overview of the experimental design for isolation, scRNA-seq, and spatial transcriptomic analysis of EC and MSC from human BM samples. **b.** UMAP representation of human BM microenvironment cells from young and elderly donors colored by cluster. Right panel: Original UMAP split into young and aged BM datasets. **c.** Dot plot of canonical markers used to define EC, MSC, and hematopoietic populations. The dot size reflects the percentage of cells within the cluster expressing each gene, and the color represents the average expression level. **d-e**. Left panel: UMAP projection of the distribution of samples for EC (d) and MSC (e). Right panel: UMAP projection of cells colored by age for EC (d) and MSC (e).

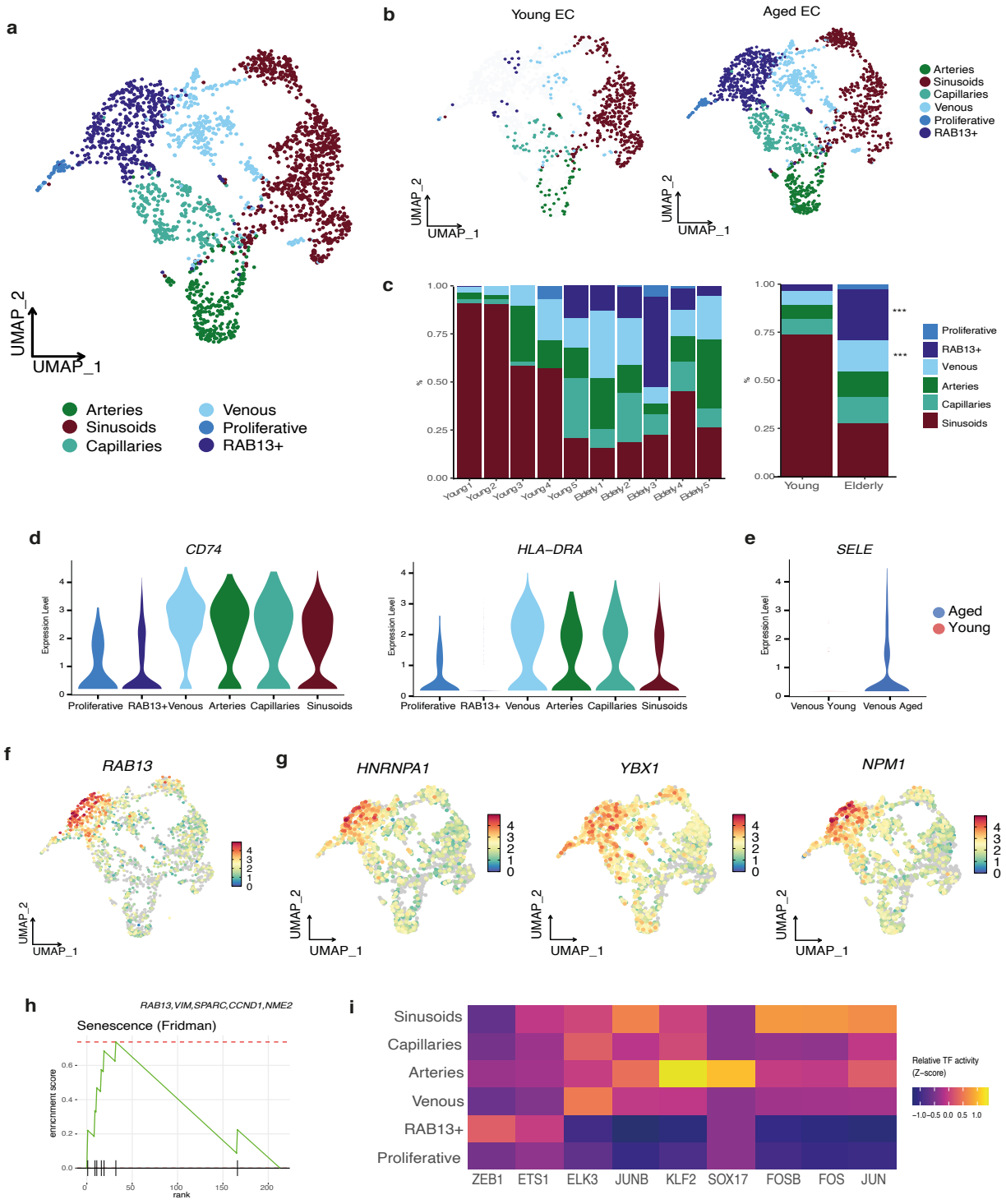

Figure 2. Aging is associated with a pro-inflammatory program in EC and emergence of RAB13^{+} senescence cells. a. UMAP depicting vascular subtypes identified within the human BM endothelial compartment. **b**. UMAP visualization of the vascular beds distribution in young (left) and aged (right) EC. **c**. Stacked bar plots showing the proportions of the different vascular states in young and aged EC per sample (left) and age group (right). Asterisks indicate significant differences in the cell proportions between the two groups (FDR < 0.05). **d.** Violin plots showing the expression of genes upregulated in the venous cluster. **e.** Violin plot displaying the expression of *SELE* in young and aged venous EC. **f**. UMAP plot revealing the gene expression of *RAB13* within EC. **g.** UMAP plots showing the expression of genes highly expressed in RAB13^{+} cells. **h**. GSEA plot of Senescence gene set enrichment in RAB13+ EC. **i**. Heatmap representing z-scaled mean regulon activity score of inferred top specific regulons for each EC vascular state.

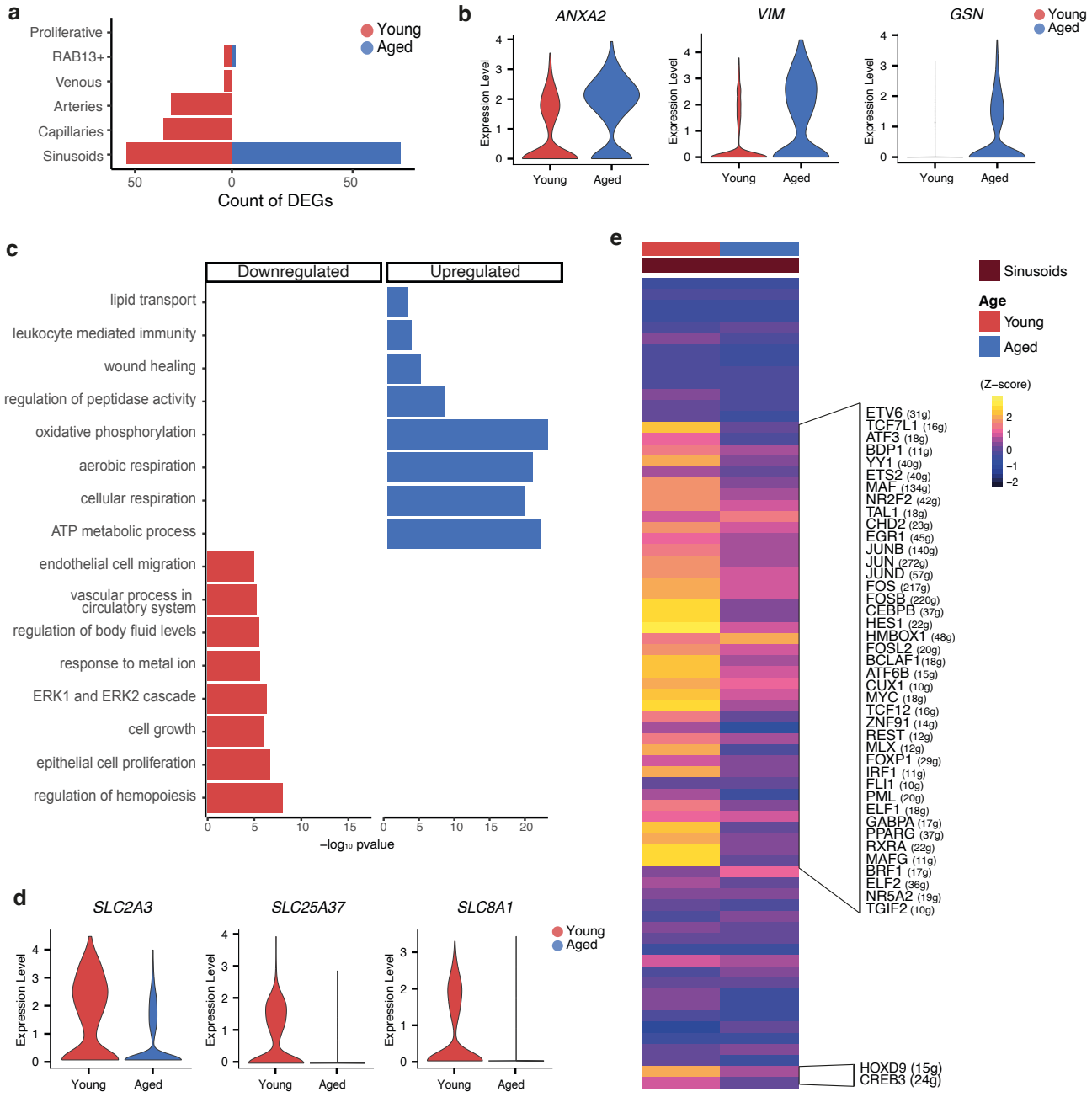

Figure 3: Aged sinusoids exhibited mitochondrial dysfunction and impaired vascular functions. a. Plot showing the number of age-related DEGs detected across vascular cell states. **b.** Violin plots of expression of *ANXA2*, *VIM,* and *GSN* in young and aged sinusoids. **c**. Bar charts of enriched GO terms from ORA (p-value < 0.05) comparing DEGs within young and aged sinusoids. The horizontal axis represents the -log10 of p-values. **d**. Violin plots of expression of solute carriers downregulated in aged sinusoids in young and aged sinusoids. **e**. Heatmap of mean regulon activity score of significantly enriched regulons in each age group within sinusoids. The color scale represents the z-score of the activity scaled by row.

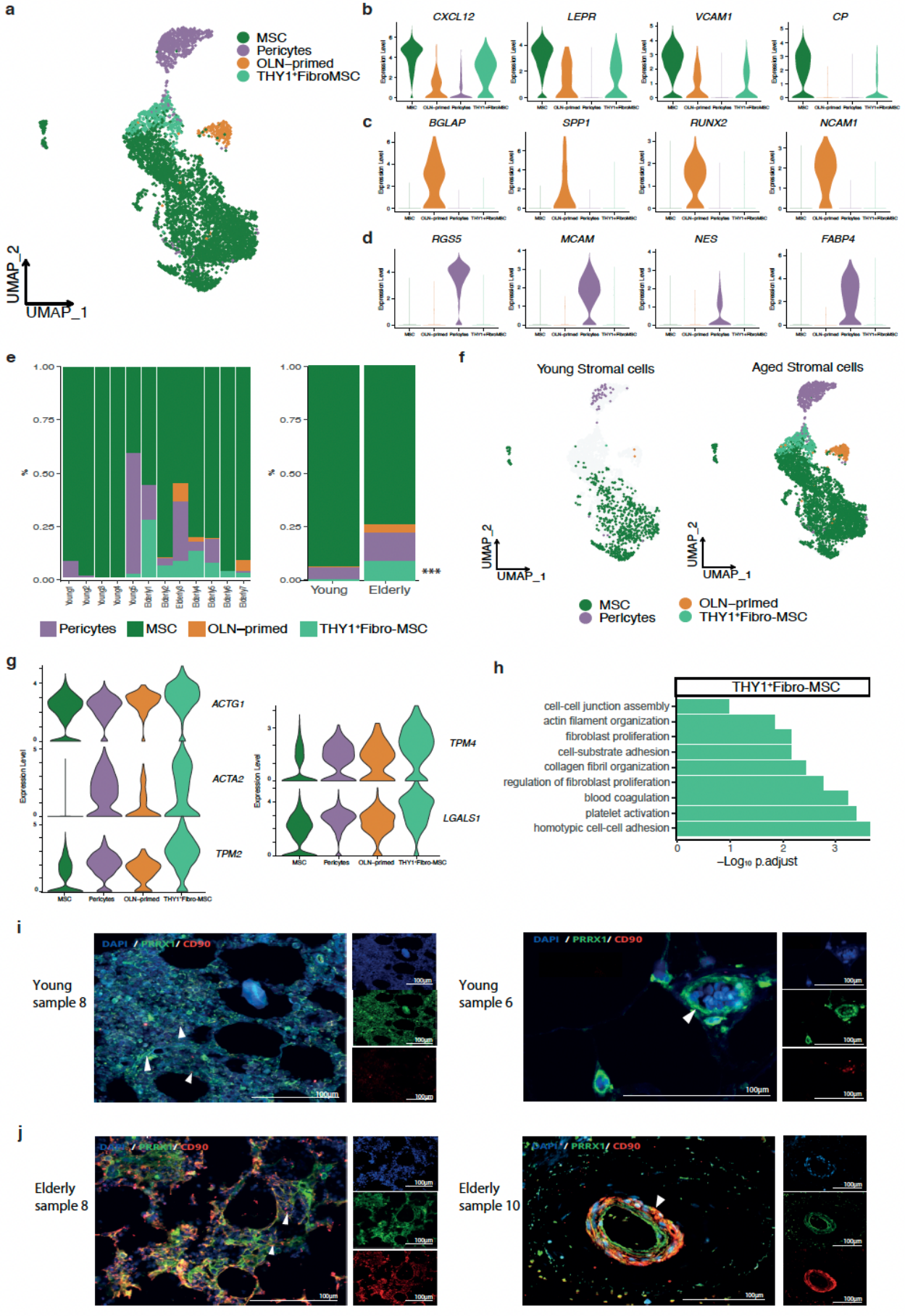
a
MSC
Pericytes
OLN–primed
THY1⁺FibroMSC
UMAP_2
UMAP_1
b
CXCL12
LEPR
VCAM1
CP
c
BGLAP
SPP1
RUNX2
NCAM1
d
RGS5
MCAM
NES
FABP4
Expression Level
e
Young
Elderly
***
Pericytes
MSC
OLN–primed
THY1⁺Fibro-MSC
f
Young Stromal cells
Aged Stromal cells
UMAP_2
UMAP_1
MSC
Pericytes
OLN–primed
THY1⁺Fibro-MSC
g
ACTG1
ACTA2
TPM2
TPM4
LGALS1
Expression Level
MSC
Pericytes
OLN-primed
THY1⁺Fibro-MSC
h
THY1⁺Fibro-MSC
cell-cell junction assembly
actin filament organization
fibroblast proliferation
cell-substrate adhesion
collagen fibril organization
regulation of fibroblast proliferation
blood coagulation
platelet activation
homotypic cell-cell adhesion
–Log10 p.adjust
i
Young sample 8
Young sample 6
DAPI / PRRX1 / CD90
100μm
j
Elderly sample 8
Elderly sample 10
DAPI / PRRX1 / CD90
100μm

Figure 4. THY1+-Fibro MSC and matrix remodeling are key factors during BM stromal aging. a. UMAP projection of the stromal cell subtypes within the human BM mesenchymal compartment. **b-d**. Violin plots showing the expression of well-known markers for MSC (b), OLN-primed (c), and pericytes (d). **e**. Stacked bar plots showing the proportions of the different stromal subtypes states in young and aged MSC per sample (left) and age group (right). Asterisks indicate significant differences in the cell proportions between the two groups. **f**. UMAP visualization of the stromal subtypes in young (left) and aged (right) MSC. **g**. Violin plot showing the expression of matrix-related genes upregulated in the THY1+Fibro-MSC cluster. **h**. Bar chart of enriched GO terms from ORA (p-value < 0.05) defining THY1+Fibro-MSC cluster. The horizontal axis represents the -log10 of adjusted p-values. **i-j**. Immunofluorescence (IF) staining of $THY1^{+}$ Fibro stromal cells ($CD90^{+}$) (red), MSC ($PRRX1^{+}$) (green), and nucleus (DAPI) (blue) in formalin-fixed paraffin-embedded (FFPE) biopsies (supplementary table 2) from two young (i) and two elderly (j) individuals. Scale bars: 100 μm.

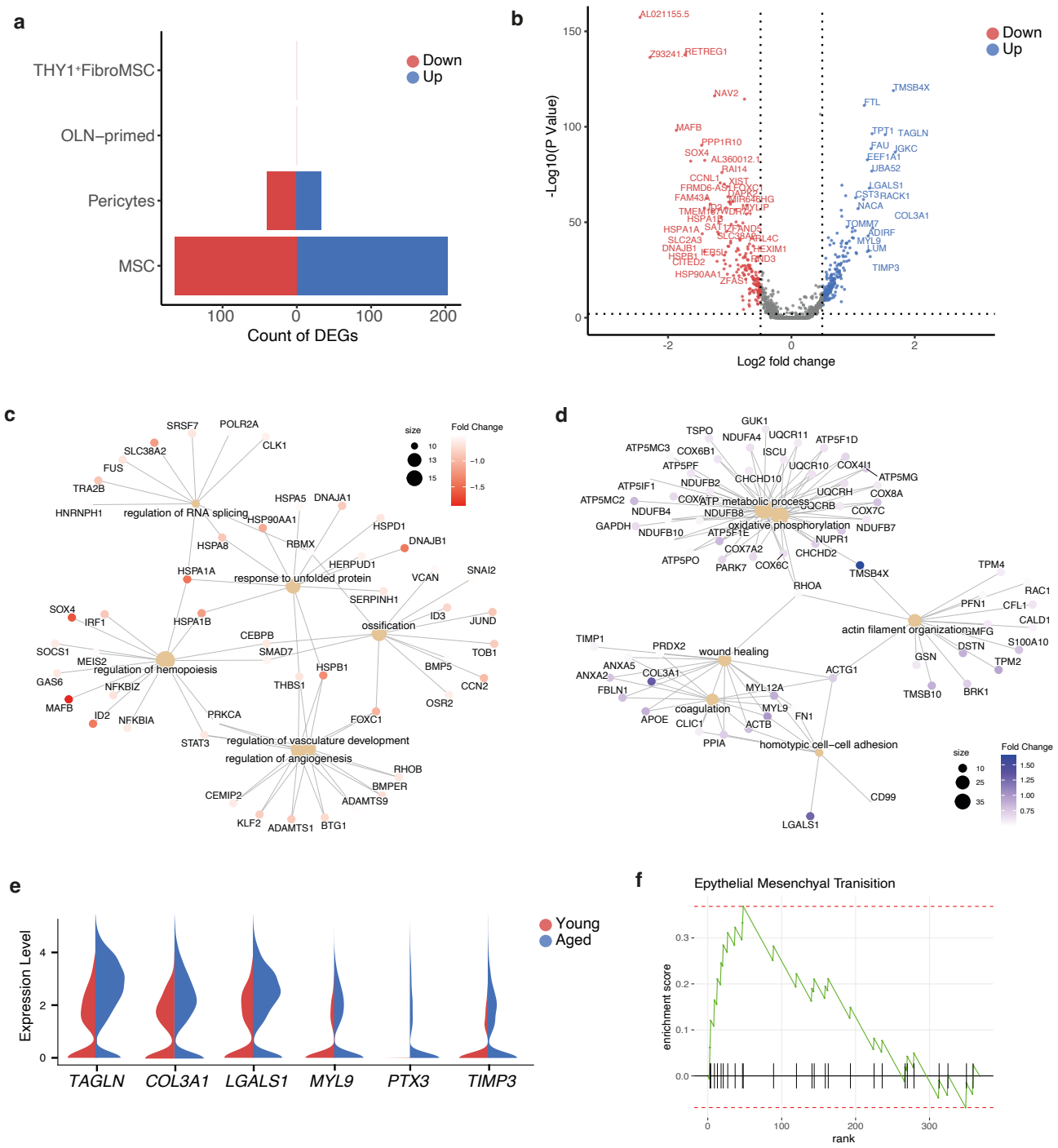

Figure 5. Impaired oxidative metabolism and protein folding capacity in aged MSC. a. Plot showing the number of age-related DEGs detected across BM stromal subpopulation. **b**. Volcano plot of the DEGs between young and aged MSC. The y-axis represents the -log10(p-value), and the x-axis represents the log2(fold change). The dot's color denotes the age group for which DEG was detected, with grey dots representing non-significant genes. **c**. Cnetplot showing the links between genes and biological processes downregulated in aged MSC. Node size reflects the number of significantly enriched genes in the node and colors the $\log_2$ Fold change expression of each gene. **d**. Cnetplot showing the relationship among individual GO terms and genes upregulated in aged MSC. Node size indicates the number of significantly enriched genes in the node and colors the $\log_2$ Fold change expression of each gene. **e**. Split violin plots showing the expression of aging-related matrix remodeling-associated genes upregulated in aged MSC. **f**. GSEA plot of "Epithelial Mesenchymal Transition" term enriched in aged MSC.

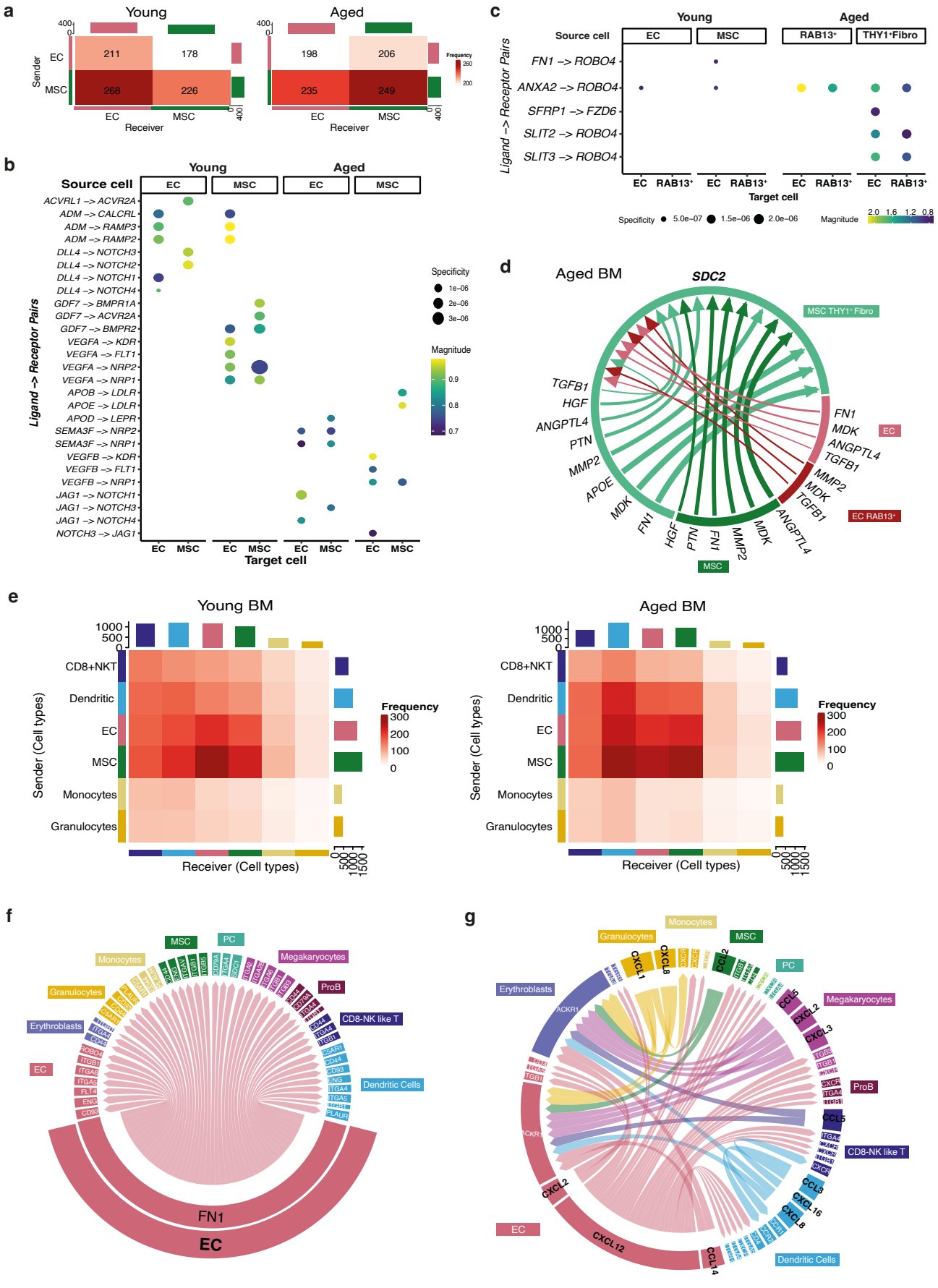
a
Young
Aged
Sender
EC
MSC
Receiver
211
178
268
226
198
206
235
249
Frequency
b
Source cell
Young
Aged
EC
MSC
Ligand -> Receptor Pairs
ACVRL1 -> ACVR2A
ADM -> CALCRL
ADM -> RAMP3
ADM -> RAMP2
DLL4 -> NOTCH3
DLL4 -> NOTCH2
DLL4 -> NOTCH1
DLL4 -> NOTCH4
GDF7 -> BMPR1A
GDF7 -> ACVR2A
GDF7 -> BMPR2
VEGFA -> KDR
VEGFA -> FLT1
VEGFA -> NRP2
VEGFA -> NRP1
APOB -> LDLR
APOE -> LDLR
APOD -> LEPR
SEMA3F -> NRP2
SEMA3F -> NRP1
VEGFB -> KDR
VEGFB -> FLT1
VEGFB -> NRP1
JAG1 -> NOTCH1
JAG1 -> NOTCH3
JAG1 -> NOTCH4
NOTCH3 -> JAG1
Target cell
Specificity
1e-06
2e-06
3e-06
Magnitude
c
Young
Aged
Source cell
EC
MSC
RAB13+
THY1+Fibro
Ligand -> Receptor Pairs
FN1 -> ROBO4
ANXA2 -> ROBO4
SFRP1 -> FZD6
SLIT2 -> ROBO4
SLIT3 -> ROBO4
Target cell
Specificity
5.0e-07
1.5e-06
2.0e-06
Magnitude
d
Aged BM
SDC2
MSC THY1+ Fibro
EC
EC RAB13+
MSC
TGFB1
HGF
ANGPTL4
PTN
MMP2
APOE
MDK
FN1
e
Young BM
Aged BM
CD8+NKT
Dendritic
EC
MSC
Monocytes
Granulocytes
Sender (Cell types)
Receiver (Cell types)
Frequency
f
MSC
PC
Monocytes
Megakaryocytes
Granulocytes
ProB
Erythroblasts
CD8-NK like T
EC
Dendritic Cells
FN1
EC
g
Monocytes
Granulocytes
MSC
PC
Erythroblasts
Megakaryocytes
ProB
CD8-NK like T
EC
Dendritic Cells
CXCL12

Figure 6. Age-related remodeling of EC-MSC communication and BM interactome. a. Heatmap illustrating predicted cellular communication between EC and MSC in young and aged BM. **b**. Dot plots representing specific ligand-receptor (L-R) interactions between EC and MSC in young and elderly donors. Dot size and color indicate the specificity and the strength of the interaction, respectively. **c**. Dot plots representing L-R communication pairs involving the RAB13^{+} EC state and THY1^{+}Fibro-MSC population in young and aged BM. Dot size and color indicate the specificity and the strength of the interaction, respectively. **d**. Chord diagram depicting age-specific communication of THY1^{+}Fibro-MSC population through *SDC2* receptor. Color represents the signal sender, and width is the strength of interactions. **e**. Heatmap illustrating predicted cellular interactions between BM microenvironment cells (EC, MSC, CD8+ NKT cells, dendritic cells, monocytes, and granulocytes) in the young (left) and aged (right) BM. Block sizes and red coloration are proportional to the number of L-R pairs. **f**. Chord diagram depicting age-specific interactions between *FN1* from EC and several proteins from different cell types. Color represents the signal sender, and width is the strength of interactions. **g**. Chord diagram showing the significant age-related signaling network between CXCL family members and other proteins from various cell types. Colors and widths represent the signal senders and the strength of interactions, respectively.

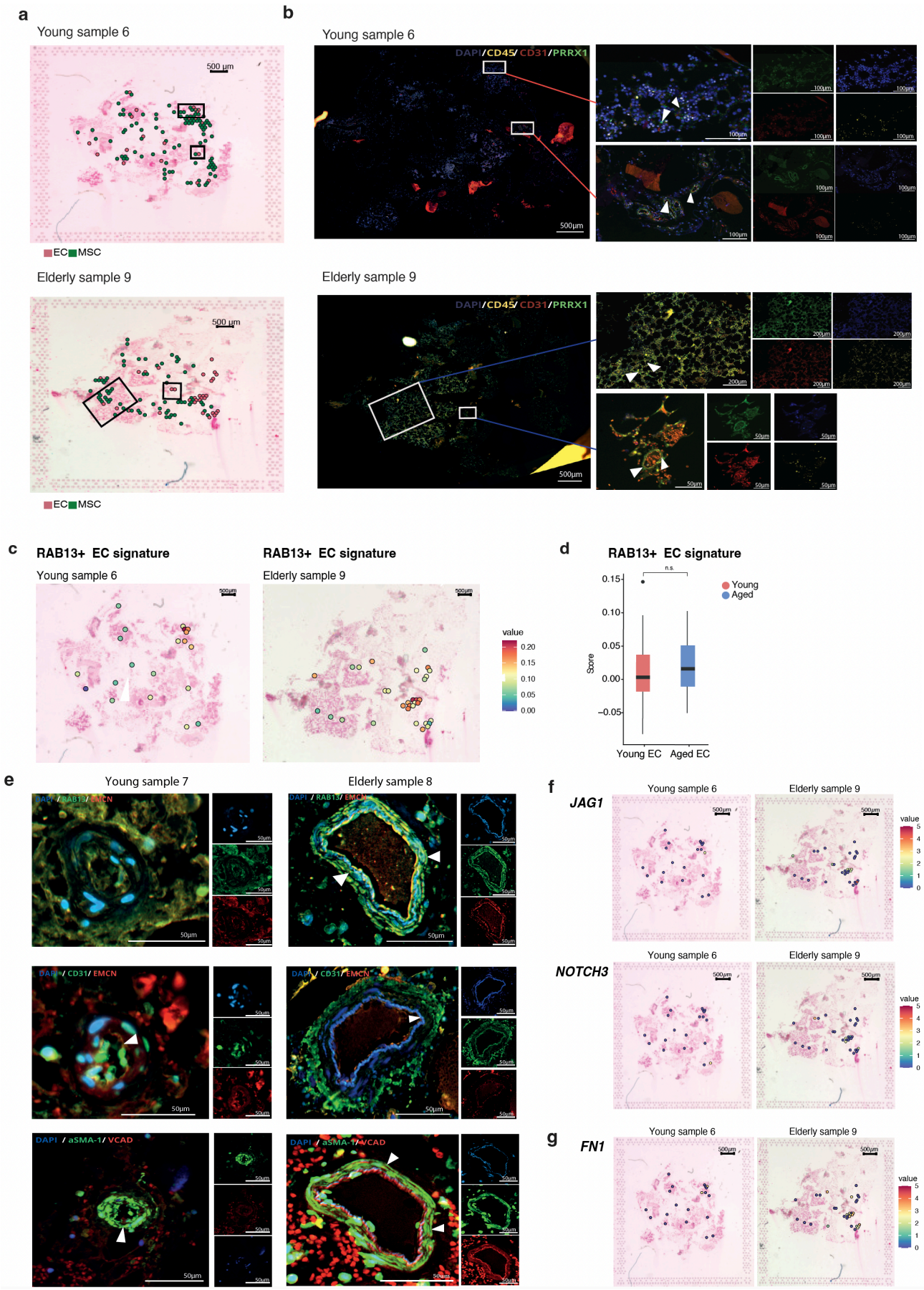
a
Young sample 6
500 µm
EC MSC
Elderly sample 9
500 µm
EC MSC
b
Young sample 6
DAPI/CD45/CD31/PRRX1
500µm
Elderly sample 9
DAPI/CD45/CD31/PRRX1
500µm
c
RAB13+ EC signature
Young sample 6
RAB13+ EC signature
Elderly sample 9
value
0.20
0.15
0.10
0.05
0.00
d
RAB13+ EC signature
n.s.
Young
Aged
Score
0.15
0.10
0.05
0.00
−0.05
Young EC
Aged EC
e
Young sample 7
Elderly sample 8
DAPI / RAB13 / EMCN
DAPI / CD31 / EMCN
DAPI / aSMA-1 / VCAD
50µm
f
JAG1
NOTCH3
Young sample 6
Elderly sample 9
value
g
FN1
Young sample 6
Elderly sample 9
value

Figure 7. Spatial transcriptomics uncovers vascular alterations along the aging process. a. Pie charts on H&E staining illustrating the proportion of each cell type highly contributing to the transcriptomic signature of each spot in young sample 6 (upper) and elderly sample 9 (bottom) new BM samples (Supplementary Table 2). **b**. IF staining of hematopoietic cells ($CD45^+$) (yellow), EC ($CD3^+$) (red), MSC ($PRRX^+$) (greeen), and nucleus (DAPI) (blue), in young (upper panels) and elderly (bottom panels) BM samples. Scale bars are indicated on each panel. **c**. Spatial expression patterns of the signature from $RAB13^+$ EC identified in scRNA-seq data in EC-labelled spots of young (left panel) and elderly (right panel) BM samples. **d**. Box plots displaying the $RAB13^+$ EC signature in young (red) and elderly (blue) EC. **e**. IF staining in the FFPE BM biopsies (supplementary table 2) of the young sample 7 (left) and elderly sample 8 (right). Scale bars: 50 µm. Upper panel: RAB13 (green), EMCN (red), and DAPI (blue). Middle panel: CD31 (green), EMCN (red), and DAPI (blue). Lower panel: αSMA1(green), VCAD (red), and DAPI (blue). **f**. Spatial expression patterns of the *JAG1-NOTCH3* L-R pair in EC golden spots of young (left panels) and elderly (right panels) BM samples **g.** Spatial expression patterns of the *FN1* ligand in EC golden spots of young (left panels) and elderly (right panels) BM samples.